Chip-Level MMSE Equalization for High-Speed Synchronous CDMA in Frequency Selective Multipath

Michael D. Zoltowski, Thomas P. Krauss, and Samina Chowdhury

School of Electrical Engineering, Purdue University
West Lafayette, IN 47907-1285
e-mail: mikedz@ecn.purdue.edu, krauss@purdue.edu, samina@ecn.purdue.edu.

ABSTRACT

This work deals with synchronous CDMA transmission using orthogonal channel codes in frequency selective multipath. The motivating application is the Forward Link in 3G CDMA Cellular Systems. In saturated systems, the intra-cell Multi-user Access Interference (MAI) created by the multipath causes the RAKE receiver to yield extremely poor performance. The chip-level MMSE estimate of the (multi-user) synchronous sum signal transmitted from the base followed by a correlate and sum with the desired user's spreading code, Walsh-Hadamard channel code multiplied by appropriate portion of long code, has been shown to yield superior performance to the RAKE receiver. This work considers reduced-rank, chip-level MMSE estimation based on the Multi-Stage Nested Weiner Filter (MSNWF) of Goldstein and Reed. It is shown that only a small number of stages of the MSNWF are needed in order to achieve near full-rank MMSE performance over a practical SNR range. This implies rapid adaptation in the case where the chip-level MMSE equalizer is adapted based on the pilot channel.

Keywords: space-time processing, smart antennas, wireless communications, CDMA, multipath propagation.

1 Introduction

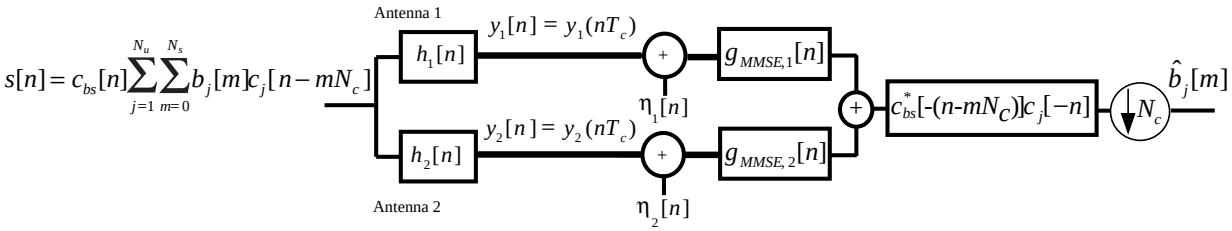

Figure 1: Chip-Level MMSE Equalization for Synchronous CDMA in Frequency Selective Multipath.

In high-speed links facilitating multimedia transmission, the multipath delay spread in urban areas may span many chips. In this case, the multipath propagation channel is frequency selective thereby negating the advantages of the orthogonality of the Walsh-Hadamard codes and creating Multi-user Access Interference (MAI) even in the case of the forward link where the users are transmitted synchronously. The resulting MAI contribution to a RAKE receiver can be quite substantial when many or all of the Walsh-Hadamard codes are being used in the same frequency band [6]. RAKE receiver here refers to a receiver that correlates and sums with the multipath distorted spreading waveform on a per symbol basis (a multipath-incorporating code-matched filter.) As a result of the multipath induced MAI, the BER curve for the RAKE receiver quickly bottoms out with increasing SNR.

However, effecting chip-level equalization on the forward link ideally restores synchronism amongst the active users allowing the chip-level equalizer to be followed by a simple correlate and sum with the desired user's spreading code [1, 2, 5, 3, 4, 8, 6]. Frank and Visotsky [1] appear to be the first published work on this basic idea; their work addresses inter-cell MAI as well as intra-cell MAI.

The mobile handset is here assumed to have two chip-spaced channels obtained through chip-rate sampling of two antennas that are either spatially separated or have distinct polarization sensitivities. Reference [4] contains a comparison of zero-forcing (ZF) equalizers and the RAKE receiver for the CDMA Forward Link. In ([6]), we derived a chip-rate MMSE equalizer that minimizes the MSE between the synchronous "sum signal" of all the users from a given base station and the equalized chip sequence; this equalizer is followed by correlation with the desired user's spreading code; see Figure 1. In this MMSE derivation, the sum of chip sequences of all the users is modeled as an i.i.d. random sequence. This leads to a "simple" chip-level MMSE equalizer that does not depend on the Walsh-Hadamard spreading codes, or the base station dependent long code. The MMSE equalizer was shown to be far superior to both ZF and RAKE.

The primary contribution of this paper is a reduced-rank, chip-level MMSE estimator based on the Multi-Stage Nested Weiner Filter (MSNWF) of Goldstein and Reed [11]. Honig and Xiao [12] have previously applied the MSNWF to the CDMA reverse link with asynchronous users, flat fading, and no long code. It was shown that only a small number of stages of the MSNWF are needed in order to achieve near full-rank MMSE performance over a practical SNR range. Simulation results presented here reveal the same is true for the CDMA forward link with synchronous users, frequency selective fading, and multiplication by the long code. This implies rapid adaptation in the case where the chip-level MMSE equalizer is adapted based on the pilot channel. The computational burden is also dramatically reduced as well.

In this paper, as in References [1],[2], [4], [5], and [6], the channel and noise power are assumed known (i.e., channel estimation error is neglected). However, as indicated in [8], where the channel is blindly estimated, channel estimation is extremely important and its failure can lead to catastrophic results for equalization. Using the exact channel in simulation and analysis leads to an informative upper bound on the performance of these methods. Frank and Visotsky [1] mention adaptive equalization based on the pilot channel, which averts the problem of estimating the channel; however, to update based on the pilot symbols, synchronization with the long code is necessary. One other important assumption made here is that the channel is unchanging which might be the case only over a short time interval. For adaptive versions of linear chip equalizers for CDMA downlink see [1] and [3] and some of the references in [5]. The most significant closed-form performance analysis we are aware of is presented in [1] in which SNR expressions are derived for the two base-station (single channel) case.

2 Data and Channel Model

The impulse response for the $i-th$ antenna channel, between the base-station transmitter and the mobile-station receiver, is

$$h_i(t) = \sum_{k=0}^{N_a-1} h_i[k] p_{rc}(t-\tau_k) \quad i = 1, 2. \tag{1}$$

$p_{rc}(t)$ is the composite chip waveform (including both the transmit and receive low-pass filters) which we assume has a raised-cosine spectrum. N_a is the total number of delayed paths or "multipath arrivals," some of which may have zero or negligible power.

In the simulation studies, we employ a realistic channel model using the software package "SMRCIM" (Simulation of Mobile Radio Channel Impulse Response Models) from Wireless Valley Communications, Inc. [7]. SMRCIM accurately models the varying types of multipath (from flat-fading to short delay spreads to very long delay spreads) encountered in an urban cellular environment, and also models the spatial correlation present in a small aperture, 2 element array.

2.1 Arrival Times and Coefficients

The channel we consider for this work consists of N_a equally spaced paths $0.625\mu s$ apart ($\tau_0 = 0$, $\tau_1 = 0.625\mu s$, ...). $h_i[k]$ may be zero or negligible for many path delays τ_k in a high-speed case where the channel is sparse. For *Channel Model 1* $N_a = 17$; this yields a delay spread of at most $10\mu s$, which is an upper bound for most channels encountered in urban cellular systems. The SMRCIM model generator, *Channel Model 2*, uses $N_a = 64$ for which $40\mu s$ is the maximum multipath delay spread; although typically the delay spread in an urban cellular environment is no more than about ten microseconds (with many channels exhibiting delay spreads of only a few microseconds or even flat fading), the presence of tall buildings or distant mountains can lead to significant channel energy at

$20\mu s$ and beyond. The spacing of $0.625\mu s$ is motivated by the software channel simulator SMRCIM which uses this spacing for urban cellular environments.

For *Channel Model 1*, we model the class of channels with 4 equal-power random coefficients with arrival times picked randomly from the set $\{\tau_0, \tau_1, \ldots, \tau_{16}\}$; the rest of the coefficients $h_i^{(1)}[k]$ are zero. Once the 4 arrival times have been picked at random and then sorted, the first and last arrival times are forced to be at 0 and the maximum delay spread of $10\mu s$, respectively. This fixes the length of the channel for this model, which guides our choice of equalizer length. The coefficients are equal-power, complex-normal random variables, independent of each other. The arrival times at antennas 1 and 2 are the same, but the coefficients are independent. See Figure 2 for a plot of a typical channel's impulse response, sampled at the chip rate.

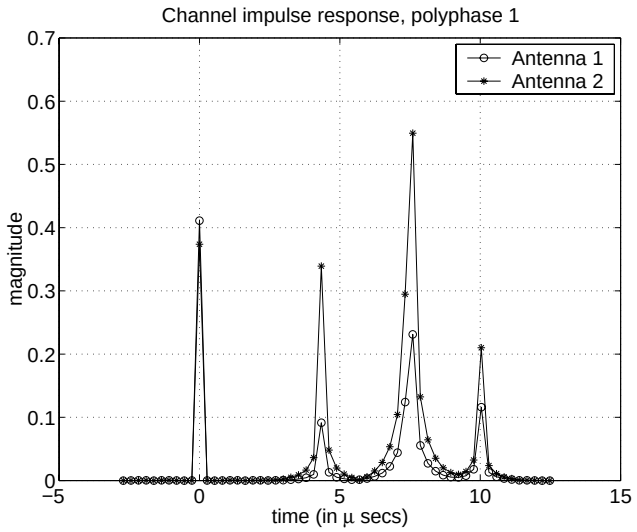

Figure 2: Typical impulse response for *Channel Model 1*, sampled at the chip rate. Includes tails from chip waveform.

For the SMRCIM channels, *Channel Model 2*, the power of the paths is random and dependent on the arrival time (with more power at earlier arrivals). See [7] for details. In Figure 3 (a) a typical, small delay spread SMRCIM channel is shown. In Figure 3 (b) a SMRCIM channel with large delay spread is shown.

2.2 Transmitted and Received Signals

The "multi-user chip symbols", $s[n]$, may be described as

$$s[n] = c_{bs}[n] \sum_{j=1}^{N_u} \sum_{m=0}^{N_s-1} b_j[m] c_j[n - N_c m] \tag{2}$$

where the various quantities are defined as follows: $c_{bs}[n]$ is the base station dependent long code; $b_j[m]$ is the $j-th$ user's bit/symbol sequence; $c_j[n]$, $n = 0, 1, ..., N_c - 1$, is the $j-th$ user's channel (short) code; N_c is the length of each channel code; N_u is the total number of active users; N_s is the number of bit/symbols transmitted during a given time window. The signal received at the $i-th$ antenna (after convolving with a matched filter impulse response having a square-root raised cosine spectrum) may be described as

$$y_i(t) = \sum_n s[n] h_i(t - nT_c) \quad i = 1, 2 \tag{3}$$

where $h_i(t)$ is defined in Eqn. (1).

In the dual antenna case, we use chip-rate sampling of the two antenna signals $y_i(t), i = 1, 2$ in Eqn. (3) to obtain the samples $y_i[n] = y_i(nT_c)$, $i = 1, 2$. The respective impulse responses are simply $h_i[n] = h_i(t)|_{t=nT_c}$, $i = 1, 2$.

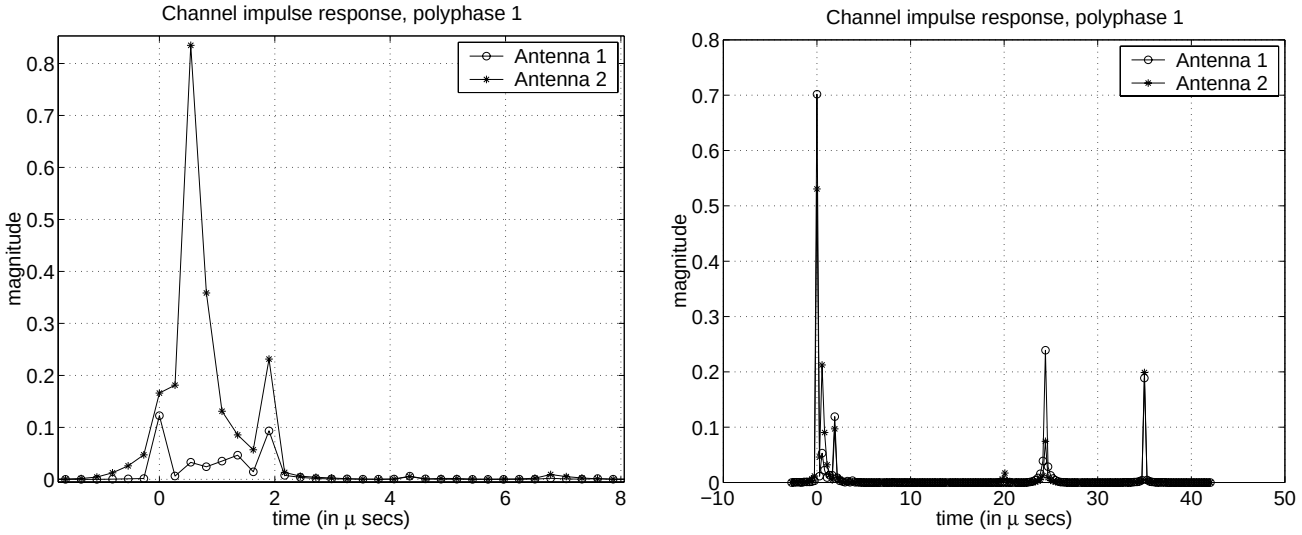

(a) Typical short delay-spread response.

(b) Typical long delay-spread response.

Figure 3: Typical chip-rate sampled impulse responses for *Channel Model 2* (SMRCIM), including chip pulse shaping.

3 ZF Equalizer Design

The synthesis of the ZF equalizing filters $g_1[n]$ and $g_2[n]$, $n = 0, 1, ..., N_g - 1$, (and used in the same configuration as the MMSE equalizers in Figure 1) is based on minimizing the output noise power subject to the ZF constraint.

$$\underset{g_1[n],\, g_2[n]}{\text{Minimize}} \quad \sum_{n=0}^{N_g-1} \{|g_1[n]|^2 + |g_2[n]|^2\}$$

$$\text{subject to:} \quad h_1[n] * g_1[n] + h_2[n] * g_2[n] = \delta[n - D] \tag{4}$$

where D is some integer chip delay. That is, ZF equalization may be effected across the two channels by combining the *chip-spaced* samples $y_i[n]$, $i = 1, 2$. Note this formulation minimizes the output noise power assuming white noise with no spatial correlation; this assumption holds for the case of two chip-spaced antenna channels, but not for the spatially correlated channels obtained by oversampling diversity. In that case, a constrained minimization of the actual noise power may be performed that takes the noise covariance into account (see the "BLUE" estimator in [3]). For our simulations we used the ZF equalizer above for both one- and two-antennas.

In matrix form, the ZF constraint may be expressed as

$$\boldsymbol{\mathcal{H}}^T \mathbf{g} = \left[\mathbf{H}_1^T \vdots \mathbf{H}_2^T\right] \begin{bmatrix} \mathbf{g}_1 \\ \mathbf{g}_2 \end{bmatrix} = \boldsymbol{\delta}_D \tag{5}$$

where $\boldsymbol{\delta}_D$ is all zeroes except for unity in the $(D+1) - th$ position and $\mathbf{H}_i$ is the $(L + N_g - 1) \times N_g$ convolution matrix

$$\mathbf{H}_i = \begin{bmatrix} h_i[0] & 0 & \dots & 0 \\ h_i[1] & h_i[0] & 0 & 0 \\ \vdots & \ddots & \ddots & \ddots \\ h_i[L-1] & h_i[L-2] & \ddots & h_i[0] \\ 0 & h_i[L-1] & \ddots & h_i[1] \\ \vdots & \ddots & \ddots & \ddots \\ 0 & 0 & 0 & h_i[L-1] \end{bmatrix}^T . \tag{6}$$

The solution is simply

$$\mathbf{g}_{ZF} = \boldsymbol{\mathcal{H}}(\boldsymbol{\mathcal{H}}^H\boldsymbol{\mathcal{H}})^{-1}\boldsymbol{\delta}_D,$$

assuming $\boldsymbol{\mathcal{H}}^T$ is square or wide, and full (row) rank. For this two channel case the matrix $\boldsymbol{\mathcal{H}}^T$ will be wide whenever the equalizer length $N_g \geq L$ the channel length. It can also be shown that $\boldsymbol{\mathcal{H}}^T$ will have full (row) rank whenever the channels do not have common zeros. To avoid conditioning problems, a small diagonal loading of 10^{-9} was applied prior to matrix inversion in the simulations.

The ZF equalizer depends on the particular delay D chosen for the right-hand side $\boldsymbol{\delta}_D$ and also the equalizer length N_g. For a fixed equalizer length, the "best choice" equalizer is the one that has smallest noise gain $\mathbf{g}^H\mathbf{g}$. It is not necessary to compute all $L + N_g - 1$ possible equalizers corresponding to each of the possible delays. Instead, we note that $\mathbf{g}_{ZF}^H\mathbf{g}_{ZF} = \boldsymbol{\delta}_D^T(\boldsymbol{\mathcal{H}}^H\boldsymbol{\mathcal{H}})^{-1}\boldsymbol{\delta}_D$ which is the $(D+1) - th$ diagonal element of $(\boldsymbol{\mathcal{H}}^H\boldsymbol{\mathcal{H}})^{-1}$. Hence our method of computing the equalizer $\mathbf{g}_{ZF}$ with the best delay is (1) compute the matrix inverse $(\boldsymbol{\mathcal{H}}^H\boldsymbol{\mathcal{H}})^{-1}$, (2) find the smallest element of the diagonal, and (3) multiply the column corresponding to that element by the matrix $\boldsymbol{\mathcal{H}}$. Our simulation experience has found that optimizing over D led to a 3-4 dB improvement in average BER performance over simply choosing $D = L$.

4 MMSE Estimate of Multi-User Synchronous Sum Signal

The MMSE equalizer is shown in Figure 1, in which an MMSE estimate of the multi-user synchronous sum signal is formed prior to correlation with the desired user's spreading code. A similar chip-level MMSE criterion is presented by Ghauri and Slock [2]; however, as in Hooli, Latva-aho, and Juntti [5], we make some simplifying assumptions to make the MMSE equalizer easier to implement. We also derive the "best delay" equalizer to improve performance. The MMSE criterion is

$$\underset{\mathbf{g}}{\text{Minimize}} \; E\{|\mathbf{g}^H(\boldsymbol{\mathcal{H}}\mathbf{s}[n] - \boldsymbol{\eta}[n]) - \boldsymbol{\delta}_D^T\mathbf{s}[n]|^2\} \tag{7}$$

where $\mathbf{s}[n]$ is a vector of $L + N_g - 1$ transmitted multi-user "chip-symbols" (the desired data), and $\boldsymbol{\eta}[n]$ is a length $2N_g$ noise vector of i.i.d. complex normal random variables with zero mean and variance σ_n^2.

As a simplifying assumption that we have found works very well in practice, we assume that the sequence values for the multi-user sum signal are i.i.d. random variables. Otherwise the covariance matrix of the sum signal $\mathbf{s}[n]$ is a complicated expression involving the Walsh-Hadamard spreading codes that varies from index to index. The i.i.d. assumption is valid if the (long) scrambling code is viewed as a random i.i.d. sequence. With this assumption, the covariance matrix of the signal is $E\{\mathbf{s}[n]\mathbf{s}[n]^H\} = \sigma_s^2\mathbf{I}$ and the MMSE equalizer can be shown to be

$$\mathbf{g}_{MMSE} = \sigma_s^2\{\sigma_s^2\boldsymbol{\mathcal{H}}\boldsymbol{\mathcal{H}}^H + \sigma_n^2\mathbf{I}\}^{-1}\boldsymbol{\mathcal{H}}\boldsymbol{\delta}_D.$$

Using a matrix inversion lemma for matrices of the form $(A + BCD)^{-1}$, this can be shown to be equivalent to

$$\mathbf{g}_{MMSE} = \sigma_s^2\boldsymbol{\mathcal{H}}\{\sigma_s^2\boldsymbol{\mathcal{H}}^H\boldsymbol{\mathcal{H}} + \sigma_n^2\mathbf{I}\}^{-1}\boldsymbol{\delta}_D.$$

This last expression shows that the MMSE equalizer gives us the best of both worlds: at low SNR, the MMSE equalizer

$$\mathbf{g}_{MMSE} \propto \boldsymbol{\mathcal{H}}\boldsymbol{\delta}_D$$

acts like the RAKE receiver, and therefore benefits from the diversity gains of the multipath-incorporating matched filter. At high SNR,

$$\mathbf{g}_{MMSE} \propto \boldsymbol{\mathcal{H}}\{\boldsymbol{\mathcal{H}}^H\boldsymbol{\mathcal{H}}\}^{-1}\boldsymbol{\delta}_D$$

acts like the ZF Equalizer and hence can completely eliminate the MAI because the orthogonality of the channel codes is restored. Note however that for channels that have close to common zeroes, the performance of the ZF equalizer does not approach the performance of the MMSE at high SNR. Because of the instability incurred in inverting the ill-conditioned matrix $\boldsymbol{\mathcal{H}}^H\boldsymbol{\mathcal{H}}$, the ZF equalizer performs much worse than the MMSE (as seen in the simulations).

As in the case of the ZF equalizer the MMSE equalizer is a function of the delay D. The MMSE is given by

$$MSE = \sigma_s^2\{1 - \sigma_s^2\boldsymbol{\delta}_D^T\boldsymbol{\mathcal{H}}^H(\sigma_s^2\boldsymbol{\mathcal{H}}\boldsymbol{\mathcal{H}}^H + \sigma_n^2\mathbf{I})^{-1}\boldsymbol{\mathcal{H}}\boldsymbol{\delta}_D\}$$

which may again be computed for each D with only one matrix inversion, which is required to form $\mathbf{g}_{MMSE}$ anyhow.

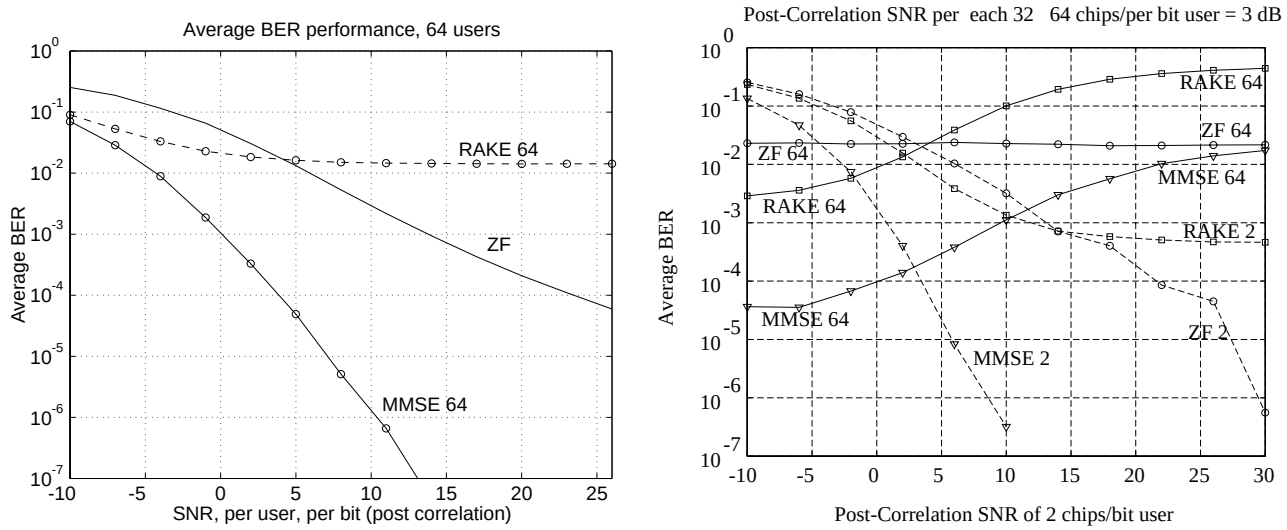

(a) 64 users (b) OVSF simulation

Figure 4: BER performance for Channel Model 1 with two antennas: RAKE vs ZF vs MMSE

5 Simulation Results

In this section, we examine through numerical simulations the performance of the three aforementioned equalizers for the CDMA downlink under conditions of frequency-selective multipath: the traditional RAKE receiver, the chip-spaced ZF equalizer, and the chip-spaced MMSE equalizer. These simulation results provide the average BER performance for users receiving from a single transmitting base-station, in which the channel is assumed static and known. We present results for the two aforementioned channel models: a random 4-path multipath channel with delay spread of 10 micro seconds, and an empirically derived random multipath channel generated by the commercial software package SMRCIM.

A wideband CDMA forward link was simulated similar to one of the options in the US cdma2000 proposal [10]. Simulations were performed for a "saturated cell," that is, all 64 possible channel codes were active. The spreading factor was $N_c = 64$ chips per bit. The chip rate was 3.6864 MHz ($T_c = 0.27\mu s$), 3 times that of IS-95. The data symbols were BPSK which, for each user, was spread with a length 64 Walsh-Hadamard function. The signals for all the users were of equal power and summed synchronously. The sum signal was scrambled with a multiplicative QPSK spreading sequence ("scrambling code") of length 32768 similar to the IS-95 standard.

BER results were obtained by averaging over many different channels and among the different users for varying SNRs. The two channel models are as previously specified in Section 2 . For Channel Model 2, SMRCIM [7] generated 100 channels at 880 MHz in an urban environment, each with distance 1 km from transmitter to receiver. Each channel consisted of 64 coefficients spaced evenly at $0.625\mu s$ apart. For two antennas, the antenna spacing was chosen as $\frac{\lambda}{4}$, which is about $8.52cm$. The "random elliptical" scattering model was employed, with a vehicle direction of 60 degrees at 3 km/hour (see [7] for details). For each trial run, a channel was chosen randomly from the 100 and the channel was generated by convolving the chip waveform with the SMRCIM impulse response and sampling at the chip-rate.

The RAKE receiver employed a maximal ratio combiner to coherently combine all the paths from both channels. The total delay of the signal, D, through both channel and equalizer, was chosen to minimize the MSE or noise gain of the equalizer for the MMSE and ZF criteria, respectively. The effects of inter-cell interference were not simulated. SNR is defined to be the ratio of the sum of the average powers of the received signals over both channels, to the average noise power, after matched filtering. Since the spreading factor (number of chips per symbol) is equal to the number of users, and each user contributes the same amount of power, this chip signal SNR is equal to the post-correlation (or de-spread) symbol-rate SNR.

The performance of the RAKE receiver is plotted in Figure 4 (a) for a "saturated cell" in which all 64 channel codes are active. Note that the abscissa in Figures 4 (a) and (b) is the **post**-correlation SNR for *each* user which

includes a processing gain of $10\log(64) \approx 18$ dB. Despite the fact that perfect channel knowledge was used, orthogonal codes were employed, the multipath delay spread was only half the symbol duration, AND there was no inter-cell interference (MAI from adjacent cells), the RAKE receiver is observed to be unable to achieve an (uncoded) BER of 10^{-2} for even very high SNR's! In fact, the reason the RAKE receiver is even able to achieve an uncoded BER of 10^{-1} is because of the ideal maximal ratio combining of the four equal strength paths at each of the two channels, giving the the RAKE receiver the benefit of a $10\log\{8\} = 9$ dB diversity gain.

In Figures 4 (a) and (b), chip-level MMSE is observed to yield performance similar to RAKE at very low SNRs, in accordance with previous analysis. At high SNR's, the MMSE equalizer substantially outperforms the ZF equalizer. This is because a small percentage of the sparse channels simulated have near common zeroes causing noise enhancement. The performance achieved with these channels dominates the BER performance of the ZF equalizer [6].

OVSF Simulation. The simulation results plotted in Figure 4 (b) reveal the substantial performance gains of a chip-level MMSE Equalizer over a RAKE receiver in the case where OVSF codes are employed. In this simulation, there were thirty-two active channel codes with 64 chips per bit plus a single 2 chips per bit channel code. Each of the thirty-two codes of length 64 employed is orthogonal to each and every integer multiple of 2 time-shift of the single code of length 2.

The post-correlation SNR for EACH of the thirty-two 64 chips per bit users (including 18 dB processing gain) was held constant equal at 3 dB. The BER performance of the RAKE receiver, chip-level MMSE equalizer, and the ZF equalizer for the single 2 chips per bit user as a function of the post-correlation SNR of the single 2 chips per bit user (including 3 dB processing gain) is plotted in Figure 4 (b) – see the curves labeled "RAKE 2", "MMSE 2", and "ZF 2", respectively. In the 3 to 10 dB SNR range, the MMSE equalizer is observed to provide several orders of magnitude improvement in uncoded BER for the single 2 chips per bit user. Note that the performance of the RAKE receiver for the 2 chips per bit user suffers from inter-symbol interference as well as multipath-induced MAI since the delay spread is 37 chips corresponding to a delay spread of roughly a half-symbol.

In addition, Figure 4 (b) plots the BER performance of the RAKE receiver, the MMSE equalizer, and the ZF Equalizer for EACH of the thirty-two 64 chips per bit users as a function of the post-correlation SNR of the single 2 chips per bit user – see the curves labeled "RAKE 64", "MMSE 64", and "ZF 64", respectively. The BER performance of the ZF equalizer for each of the thirty-two 64 chips per bit users is observed to remain relatively constant as the SNR of the single 2 chips/bit user is increased due to the restoration of channel code orthogonality. In contrast, the BER performance of the RAKE receiver for each of the thirty-two 64 chips per bit users is observed to increase dramatically as the SNR of single 2 chips per bit user is increased, since this increases the level of the MAI affecting each of the thirty-two 64 chips per bit users.

As the SNR of the single 2 chips per bit user is increased, the point at which the BER of the single 2 chips per bit user is the same as that for EACH of the thirty-two 64 chips per bit users occurs at roughly the same SNR for all three different methods. Interestingly, this cross-over point occurs when the post-correlation SNR (includes 3 dB processing gain) of the single 2 chips per bit user is equal to the post-correlation SNR (includes 18 dB processing gain) of EACH of the thirty-two 64 chips per bit users: 3 dB. However, the BER at this cross-over point achieved with the chip-level MMSE equalizer is two orders of magnitude lower than the cross-over point BER achieved with either the RAKE receiver or ZF equalizer. These simulation results are a strong testament to the efficacy of employing an MMSE based chip-level equalization in the case of synchronous CDMA with OVSF channel codes.

5.1 Dual Antenna versus Single Antenna at Receiver.

In the case of a single antenna, two channels may be realized by sampling at twice the chip-rate to obtain $y_1[n] = y_1(nT_c)$ and $y_2[n] = y_1(\frac{T_c}{2} + nT_c)$. These respective impulse responses for the two corresponding polyphase channels $h_1[n] = h_1(t)|_{t=nT_c}$ and $h_2[n] = h_1(t)|_{t=\frac{T_c}{2}+nT_c}$. For Channel Model 1, two equalizer lengths per polyphase (or antenna) channel were simulated: 57 chips, which is equal to the channel length, and 114 chips. For Channel Model 2 (SMRCIM), a length 100 equalizer was used. This is shorter than the maximum channel length but is sufficiently long to allow exact (ZF) inversion for most channels (provided the channels have no common-nulls). The MMSE simulation results are shown in Figures 5 (a) and 5 (b) along with the RAKE results for comparison. Figure 5 (a) and (b) show the mean BER for Channel Models 1 and 2, respectively. Note that each abscissa value is the post-correlation SNR of a single user at a given receive antenna; that is, it includes the channel gains as well as the processing gain.

The average BER results indicate that for all three types of equalizers, a dual antenna receiver offers a significant

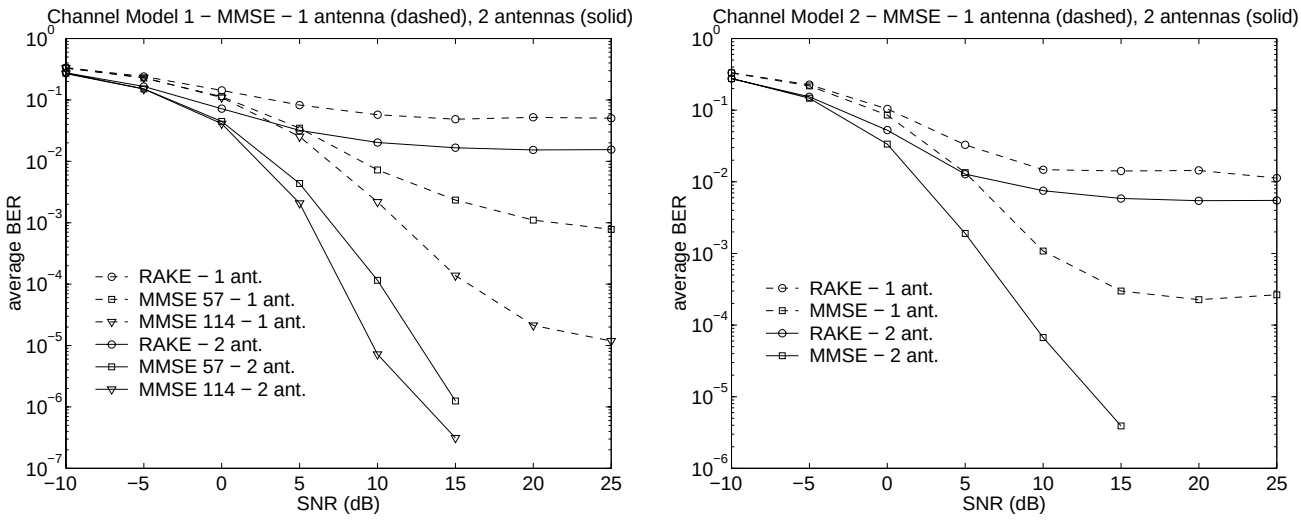

(a) Channel Model 1. (b) Channel Model 2.

Figure 5: Average BER performance of MMSE and RAKE receivers.

performance improvement over creating two channels via oversampling at a single antenna. However, in the saturated cell scenario, the RAKE receiver does not benefit from the additional antenna as substantially as the MMSE equalizer. Finally, both ZF and MMSE perform better when the equalizer length is doubled.

5.2 MSNWF Applied to Synchronous CDMA in Frequency Selective Multipath

There has been much work on reduced-rank adaptive filtering schemes that constrain the adaptive weight vector to lie in a low-dimensional subspace. This substantially reduces the computational burden and dramatically speeds up convergence, if the subspace is chosen properly. In linear Minimum Mean Square Error (MMSE) estimation, the optimum weight vector is the solution to the Weiner-Hopf equation

$$\mathbf{R}_{xx}\mathbf{w} = \mathbf{r}_{dx} \tag{8}$$

where $\mathbf{R}_{xx}$ is the correlation matrix of the data and $\mathbf{r}_{dx}$ is the cross-correlation vector between the data and the desired signal. For the chip-level MMSE equalizer, $\mathbf{R}_{xx} = \sigma_s^2 \boldsymbol{\mathcal{H}}\boldsymbol{\mathcal{H}}^H + \sigma_n^2\mathbf{I}$ and $\mathbf{r}_{dx} = \boldsymbol{\mathcal{H}}\boldsymbol{\delta}_D$. Prior work along the lines of dimensionality reduction restricted the weight vector $\mathbf{w}$ to lie in a subspace spanned by the Principal Components (PC) or dominant eigenvectors of $\mathbf{R}_{xx}$. Although this speeds up convergence, there is the intense computational burden of computing the dominant eigenvectors of $\mathbf{R}_{xx}$.

Goldstein and Reed formulated an alternative to Principal Components analysis referred to as the Multi-Stage Nested Weiner Filter (MSNWF) [11]. The MSNWF represents a pioneering breakthrough in that it achieves a convergence speed-up substantially better than that achieved with Principal Components at a dramatically reduced computational burden relative to Principal Components. Intuitively speaking, achieving the best of both worlds – faster convergence AND reduced computation – is made possible by making use of the information inherently contained in both $\mathbf{R}_{xx}$ and $\mathbf{r}_{dx}$ in choosing the reduced-dimension subspace $\mathbf{w}$ is constrained to lie within. In contrast, Principal Components only makes use of the information embedded in $\mathbf{R}_{xx}$.

In MSNWF, there is no computation of eigenvectors. Honig and Xiao [12] have shown that if the MSNWF is terminated at stage D, the weight vector is constrained to lie in the Krylov subspace spanned by $\{\ \mathbf{r}_{dx},\ \mathbf{R}_{xx}\mathbf{r}_{dx},\ \mathbf{R}_{xx}^2\mathbf{r}_{dx},\ \ldots\ ,\ \mathbf{R}_{xx}^{D-1}\mathbf{r}_{dx}\ \}$. Through theoretical analysis and extensive supporting simulations, MSNWF has been shown to achieve near optimal SINR performance with a subspace of dimension roughly equal to $D = 8$ or less under diverse operating conditions for two different applications: (1) cancellation of multi-user access interference (MUAI) in asynchronous CDMA with flat fading [12] and (2) cancellation of narrowband/wideband jammers for GPS employing a power minimization based space-time pre-processor [13]. The fact that a subspace of dimension only equal to roughly $D = 8$ provides near optimal SINR performance in two very different application areas is an astounding result that motivates application of MSNWF to synchronous CDMA in frequency selective multipath.

The MSNWF algorithm is summarized below and depicted in Figure 6. $\mathbf{x}(n)$ is a block of chip-level data which has the same dimension as the equalizing vector $\mathbf{g}$ defined previously.

- *Initialization:* $d_0(n) = d(n)$ and $\mathbf{x}_0(n) = \mathbf{x}(n)$
- *Forward Recursion:* For $k = 1, 2, ..., D$:

$$\begin{aligned} \mathbf{p}_k &= E\{d_{k-1}^*(n)\mathbf{x}_{k-1}(n)\}/||E\{d_{k-1}^*(n)\mathbf{x}_{k-1}(n)\}|| \\ d_k(n) &= \mathbf{p}_k^H \mathbf{x}_{k-1}(n) \\ \mathbf{B} &= \mathbf{I} - \mathbf{p}_k\mathbf{p}_k^H \\ \mathbf{x}_k(n) &= \mathbf{B}\mathbf{x}_{k-1}(n) \end{aligned} \tag{9}$$

- *Backward Recursion:* For $k = D, D-1, ..., 1$, with $\epsilon_D(n) = d_D(n)$:

$$\begin{aligned} w_k &= E\{d_{k-1}^*(n)\epsilon_k(n)\}/E\{|\epsilon_k(n)|^2\} \\ \epsilon_{k-1}(n) &= d_{n-1}(n) - w_k^*\epsilon_k(n) \end{aligned} \tag{10}$$

It is easily shown that

$$\mathbf{p}_{k+1} = \frac{(\mathbf{I} - \mathbf{p}_k\mathbf{p}_k^H)\mathbf{R}_{k-1}\mathbf{p}_k}{||(\mathbf{I} - \mathbf{p}_k\mathbf{p}_k^H)\mathbf{R}_{k-1}\mathbf{p}_k||} \tag{11}$$

where

$$\mathbf{R}_{k+1} = (\mathbf{I} - \mathbf{p}_{k+1}\mathbf{p}_{k+1}^H)\mathbf{R}_k(\mathbf{I} - \mathbf{p}_{k+1}\mathbf{p}_{k+1}^H) \tag{12}$$

for $k = 0, 1, ..., D-1$, where $\mathbf{p}_1 = \mathbf{r}_{dx}$ and $\mathbf{R}_0 = \mathbf{R}_{xx}$. It follows that the matrix $\mathbf{T}_D = [\mathbf{p}_1\ \mathbf{p}_2\ ...\ \mathbf{p}_D]$ contains orthonormal columns and that the reduced dimension $D \times D$ correlation matrix $\mathbf{T}_D^H\mathbf{R}_{xx}\mathbf{T}_D$ is tri-diagonal [11, 12].

Figure 7 plots the MSE of the MSNWF as a function of subspace dimension, D, or rank of the dimensionality reducing matrix transformation, i.e., the stage at which the MSNWF is terminated. The dimension of the full space is 114: there's an equalizing filter of length 57 chips at each of the two antennas; this encompasses the multipath delay spread of 37 chips (corresponding to 10 μs) plus 10 chips worth of chip pulse shaping (5 on either side). The subspace dimension at which MSNWF approximately achieves the performance of the full-dimension ideal (asymptotic) Weiner filter is roughly around 5! In contrast, Principal Components (PC) generally requires a subspace dimension equal to roughly twice the delay spread (in units of chips).

Note that Figure 7 also displays the performance of the Cross-Spectral Metric (CSM) method [14]. Similar to the PC method, the CSM method constrains the equalizing filter vector to lie in a subspace spanned by a subset of the eigenvectors of the correlation matrix. The choice of eigenvectors is dictated by a cross-spectral metric derived from the cross-correlation vector, rather than simply choosing those eigenvectors associated with the largest eigenvalues. CSM yields improved performance relative to PC, but its performance is not nearly as good as MSNWF and it too requires the computation of eigenvectors. Again, there is no computation of eigenvectors involved in the MSNWF. Only a small number of simple matrix-vector multiplications are required. In contrast, the computation of the 80 or so eigenvectors needed by the PC method is a substantial computational burden.

Figure 8 displays the BER curves obtained with the MSNWF employing Channel Model 1 for different sizes of the reduced-dimension subspace. That is, Figure 8 displays the BER curve obtained when the MSNWF is terminated at stage 1 for each channel, the BER curve obtained when the MSNWF is terminated at stage 2 for each channel, etc. It is observed that only a small number of stages of the MSNWF are needed in order to achieve near full-rank MMSE performance over a practical range of SNR's. The results show that the BER curve obtained stopping at stage 5 is nearly coincident with the full rank MMSE solution over the range of SNR actual systems operate within in practice. This implies rapid adaptation in the case where the chip-level MMSE equalizer is adapted based on the pilot channel.

ACKNOWLEDGEMENTS

This research was supported by the Air Force Office of Scientific Research under grant no. F49620-97-1-0275, the National Science Foundation under grant no. MIP-9708309, and Texas Instruments' DSP University Program.

References

[1] Colin D. Frank and Eugene Visotsky, "Adaptive Interference Suppression for Direct-Sequence CDMA Systems with Long Spreading Codes", *in Proceedings 36th Allerton Conf. on Communication, Control, and Computing*, pp. 411–420, Monticello, IL, Sept. 23-25 1998.

[2] I. Ghauri and DTM. Slock, "Linear receivers for the DS-CDMA downlink exploiting orthogonality of spreading sequences", *Conf. Rec. 32rd Asilomar Conf. on Signals, Systems, & Comps., Pacific Grove, CA,*, Nov. 1998.

[3] S. Werner and J. Lilleberg, "Downlink Channel Decorrelation in CDMA Systems with Long Codes", *in Proc. Vehicular Technology Conference (VTC '99)*, Houston, TX, May 5-9 1999.

[4] M. Zoltowski and T. Krauss, "Two-Channel Zero Forcing Equalization on CDMA Forward Link: Trade-offs between Multi-user Access Interference and Diversity Gains", *in Conf. Rec. 33rd Asilomar Conf. on Signals, Systems, and Computers, Pacific Grove, CA*, Oct. 25-27 1999.

[5] Kari Hooli, Matti Latva-aho, and Markku Juntti, "Multiple Access Interference Suppression with Linear Chip Equalizers in WCDMA Downlink Receivers", *in Proc. Global Telecommunications Conf.*, pp. 467–471, Rio de Janero, Brazil, Dec. 5-9 1999.

[6] T. Krauss, M. Zoltowski and G. Leus, "Simple MMSE Equalizers for CDMA Downlink to Restore Chip Sequence: Comparison to Zero-Forcing and RAKE", *in International Conference on Acoustics, Speech, and Signal Processing*, June 5-9 2000.

[7] Wireless Valley Communications, Inc., *SMRCIM Plus 4.0 (Simulation of Mobile Radio Channel Impulse Response Models) User's Manual*, Aug. 24 1999.

[8] T. Krauss and M. Zoltowski, "Blind Channel Identification on CDMA Forward Link Based on Dual Antenna Receiver at Hand-set and Cross-relation", *Conf. Rec. 33rd Asilomar Conf. on Signals, Systems, and Computers, Pacific Grove, CA,*, Oct. 25-27 1999.

[9] T. P. Krauss and M. D. Zoltowski, "Oversampling diversity versus dual antenna diversity for chip-level equalization on CDMA downlink," *First IEEE Sensor Array and Multichannel Signal Processing Workshop,* Cambridge, Massachusetts, 16-17 March 2000.

[10] Telecommunications Industry Association, "Physical Layer Standard for cdma2000 Spread Spectrum Systems - TIA/EIA/IS-2000-2", TIA/EIA Interim Standard, Aug. 1999.

[11] J. S. Goldstein, I. S. Reed, and L. L. Scharf, "A Multistage representation of the Weiner filter based on orthogonal projections," *IEEE Trans. Information Theory*, Vol. 44, No. 7, pp. 2943-2959, Nov. 1998.

[12] M. L. Honig and W. Xiao. "Large system performance of reduced-rank linear interference suppression for DS-CDMA." In *Proc. Allerton Conf. on Comm., Control, and Computing*, Monticello, IL, October 1999.

[13] W. Myrick, M. D. Zoltowski and J. S. Goldstein, 'Anti-Jam Space-Time Preprocessor for GPS Based on Multistage Nested Wiener Filter," *IEEE Military Communications (Milcom '99),* Atlantic City, NJ, 3-6 Oct. 1999.

[14] J. S. Goldstein and I. S. Reed, "Subspace selection for partially adaptive sensor array processing," *IEEE Trans. Aerospace and Electronic Systems*, Vol. 33, No. 2, pp. 539-544, April 1997.

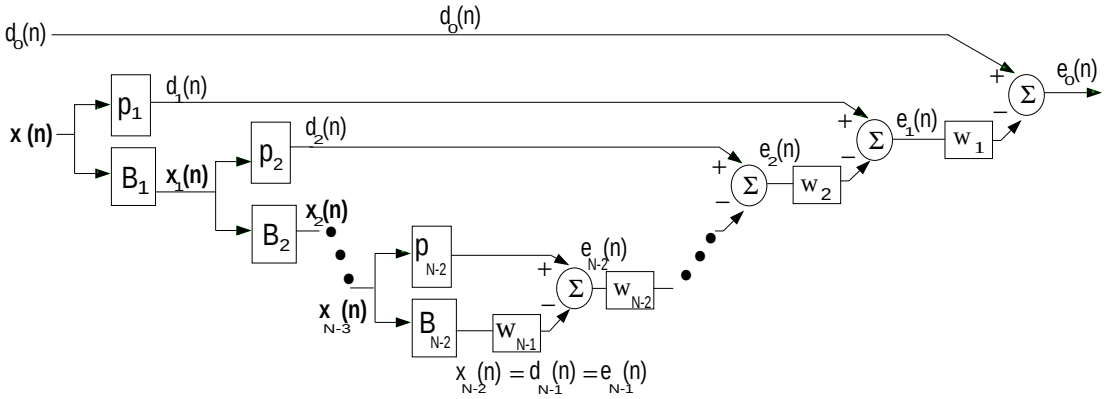

Figure 6: Structure of successive stages of the Multistage Nested Weiner Filter.

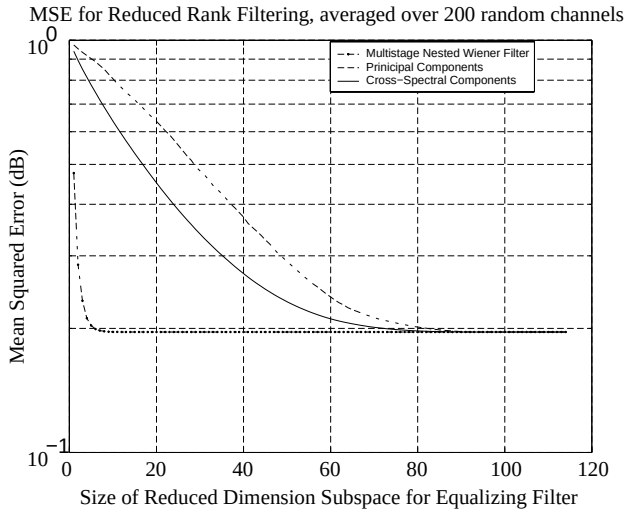

Figure 7: MSE vs size of reduced dimension Subspace: MSNWF vs PC vs CSM.

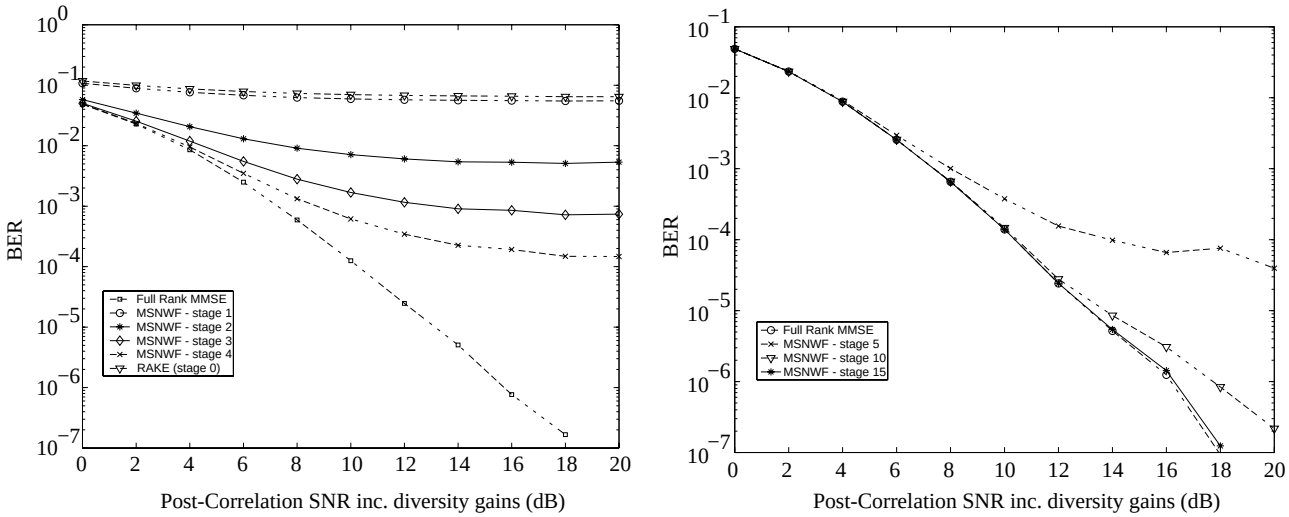

Figure 8: BER of MSNWF with Channel Model 1 for different subspace dimensions.